Effective Hamiltonian Models and Unimolecular Decomposition[†]

Curt Wittig* and Ilya Bezel[‡]

Department of Chemistry, University of Southern California, Los Angeles, California 90089

Received: March 24, 2006; In Final Form: May 24, 2006

Partitioning Hilbert space into two subspaces by using orthogonal projection operators yields compact forms for effective Hamiltonians for each of the subspaces. When one (the Q space) contains molecular bound states and the other (the P space) contains dissociative continua, a simple form for the non-Hermitian Q-space effective Hamiltonian, H^{eff}, can be obtained, subject to reasonable approximations. Namely, $H^{eff} = H^0 - i\hbar\Gamma/2$, where H^0 is Hermitian, and the width operator $\hbar\Gamma$ accounts for couplings of the Q-space levels to the P-space continua. The P/Q partitioning procedure has been applied in many areas of atomic, molecular, and nuclear physics with widespread success. Inputting into this formalism ideas from random matrix theory in order to model independent open channels yields the random matrix H^{eff} model. Despite numerous efforts, this model has failed to model satisfactorily the statistical transition-state theory of unimolecular decomposition (hereafter referred to as TST) in the regime of overlapping resonances, where nearly all such reactions occur. All statistical models of unimolecular decomposition are premised on rapid intramolecular vibrational redistribution (IVR) for a given set of good quantum numbers. The phase space thus accessed results in a threshold reaction rate of $1/h\rho$, and for K independent open channels, the rate is $K/h\rho$. This reaction rate corresponds to a resonance width of $K/2\pi\rho$, and when K increases, the resonances (which are ρ^{-1} apart) overlap. In this regime, the random matrix H^{eff} model fails because it does not introduce independent open channels. To illustrate the source of the problem, an analysis is carried out of a simple model that is obviously and manifestly inconsistent with TST. This model is solved exactly, and it is then put in the form of the random matrix H^{eff} model, illustrating the one-to-one correspondence. This reveals the deficiencies of the latter. In manipulating this model into the form $H^0 - i\hbar\Gamma/2$, it becomes clear that the independent open channels in the random matrix H^{eff} model are inconsistent with TST. Rather, this model is one of gateway states (i.e., bound states that are coupled to their respective continua as well as to a manifold of zero-order bound states, none of which are coupled directly to the continua). Despite the fact that the effective Hamiltonian method is, by itself, beyond reproach, the random matrix H^{eff} model is flawed as a model of unimolecular decomposition in several respects, most notably, bifurcations of the distributions of resonance widths in the regime of overlapping resonances.

I. Introduction and Background

Some time ago,[1−3] Miller and Moore introduced a model for unimolecular decomposition that deals with quantum mechanical phenomena beyond the purview of microcanonical transition-state theories such as RRKM (Rice, Ramsperger, Kassel, and Marcus), PST (phase space theory), and SACM (statistical adiabatic channel model).[4,5] It focuses on resonances that derive from couplings between bound rovibronic levels and dissociative continua of independent open reactive channels, resulting in quasibound levels. In an earlier, influential paper by Mies and Krauss, unimolecular decomposition had been analyzed in terms of resonance decay in the regime where the resonances overlap, i.e., their widths exceed their average separation.[6]

Before proceeding, it is useful to clarify what is meant by independent open channels and associated dissociative continua. In the statistical theory of unimolecular reactions, independent open channels are accessed via corresponding transition-state (TS) levels, as indicated in Figure 1. These TS levels are the thresholds for the open channels. For reactions in which
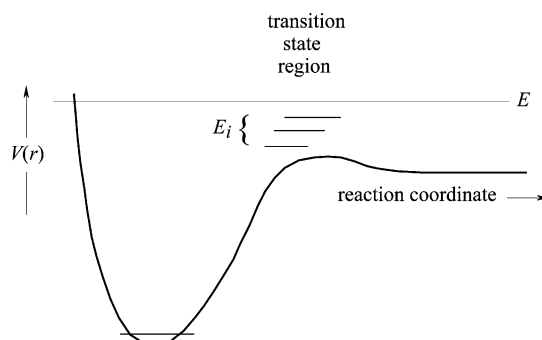
Figure 1. Energies of the transition state (TS) levels (i.e., the channel thresholds) are denoted E_i. For a given TS level, the translational energy in the TS region is approximately constant at $E - E_i$. The independent open channels accessed via their TSs extend into their continua.

dissociation occurs (as opposed to isomerization), each independent open channel leads to fragments that lie in the channel's dissociation continuum. An independent open channel is not, in general, equivalent to a single resolved product state, i.e., a set of quantum numbers for the fragments. It originates at its TS region and from there *evolves* to a set of product quantum states. Thus, accessing a TS level is equivalent to accessing

Effective Hamiltonian Models

J. Phys. Chem. B, Vol. 110, No. 40, 2006 **19851**

the corresponding open channel. The TS region lies along the reaction coordinate at a location that separates the parent and product spaces.

In the model of Miller and Moore, statistical properties of wave functions, resonance widths, spectral intensities, and so forth are justified on the basis of physical arguments, and ideas from random matrix theory[7,8] are enlisted. The statistical analyses are based on seminal work of Porter and Thomas[9,10] that reconciled experimental data in the field of nuclear physics. Specifically, fluctuations (i.e., erratic changes from one reso-nance to the next) had been noted for widths associated with the following: (i) low-energy neutron capture by heavy target nuclei, (ii) fission, and (iii) radiation. Previous work by Hughes and Harvey had shown, through a compilation of most of the available data, that the widths for (i) could be fitted to a χ-squared distribution having between one and two degrees of freedom. In this work, the term "degrees of freedom" referred to the mathematical form of the χ-squared distribution.[11] Later, Miller and Moore showed that these degrees of freedom are equivalent to independent open channels. Though the original fit was empirical, analyses by Porter and Thomas[9] provided a theoretical explanation of the experimental results, as well as a basis for making predictions. Extension of their model to unimolecular reactions is straightforward.

In the 1980s, laser and nozzle expansion techniques enabled experimental studies of unimolecular decomposition to be carried out at the state-to-state level. The first system to be examined thoroughly was NCNO → CN + NO, which adheres to standard statistical models.[12] On the other hand, for D_2CO → D_2 + CO, it was observed that decay widths of individual resonances, as well as coupling matrix elements between S_0 and S_1, fluctuate over a modest energy interval.[13−16] This was attributed to the nature of the S_0 eigenstates and their corre-sponding resonances. Namely, chaotic vibrational dynamics give rise to eigenstates whose projections on the reaction coordinate differ significantly from one level to the next. Expansion coefficients of the S_0 eigenstates in a separable Hamiltonian basis are random, subject to normalization.

Virtues of the model include the fact that it is simple and not system-specific. Unlike other models, it deals with quantum fluctuation phenomena that have been observed in highly resolved experimental studies. This work has advanced our understanding of unimolecular reactions.

For bound Hamiltonian systems in the chaotic regime, Wigner derived a simple formula for the distribution of nearest-neighbor spacing for levels having the same good quantum numbers[7]

$$P_W(s) = \frac{\pi}{2} s \exp\left(-\frac{\pi}{4} s^2\right) \tag{1}$$

where s is the normalized spacing between adjacent levels (i.e., the spacing divided by the average spacing) and $P_W(s)$ is the probability density. Equation 1 is not system-specific. It can be applied to disparate phenomena, ranging from the quasi-bound levels of excited nuclei (prepared by the capture of low-energy neutrons by heavy nuclei) to the vibrational levels of polyatomic molecules.

Random matrix theory, also introduced by Wigner,[17−19] provides a rigorous derivation of the level statistics for the Gaussian orthogonal ensemble (GOE) of asymptotically infinite, real, symmetric, random matrices and yields a result that is close to eq 1, albeit not in closed form.[7] In addition, it provides statistical measures for higher-order correlations, the most common being the Δ_3 statistic of Dyson and Mehta.[20,21] Though the derivation of the GOE result is more formal than the original
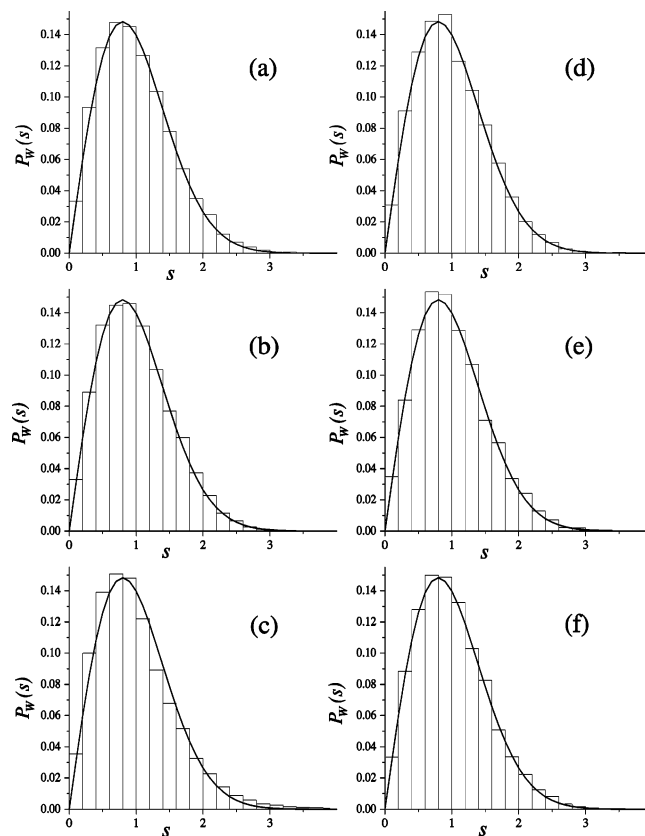
Figure 2. Nearest-neighbor spacing distributions, obtained by matrix diagonalization, that demonstrate the robustness of eq 1. The matrices are of dimension 2000, and the average nearest-neighbor spacing is 1. In (a−c), the diagonal elements have been obtained by using (a) a Wigner distribution (i.e., $P_W(s)$, eq 1); (b) equal spacing; and (c) a Poisson distribution (i.e., $P_P(s) = e^{-s}$), and H_{ij} that have been chosen randomly from a Gaussian normal distribution with $\sigma^2 = 1$ and a mean of zero. In (d−f), the diagonal elements are the same as in (a−c), but the H_{ij} have been chosen randomly from a Gaussian normal distribution with $\sigma^2 = 10$. To avoid effects from the matrix boundaries, only states with $-500 < E < 500$ have been used in the histograms. All results are averaged over 10 matrices. The solid lines are Wigner distributions $P_W(s)$.

derivation given by Wigner for eq 1, there is little difference in content. Equation 1 can be readily subsumed into models of unimolecular processes in which the dynamics are assumed to be chaotic in the region of bound states.

A Hamiltonian system whose energy-level spacing distribu-tion is in agreement with eq 1 can be said to be quantum chaotic. Classical chaos can be defined by exponential divergence from one another of nearby trajectories in phase space. As no such definition is available for the quantum counterpart, we take eq 1 as an ad hoc definition. In this regime, adding reasonable off-diagonal matrix elements does not change the nature of the dynamics. For example, suppose a diagonal matrix obeys eq 1. Adding reasonable off-diagonal matrix elements changes the eigenvalues, but the distribution of eigenvalues still obeys eq 1, as illustrated in Figure 2. Thus, the chaotic nature of the dynamics is robust. Note that an ergodic system (one that fills the phase space) is not necessarily chaotic. As used here, chaos is a trait of the system's dynamics. It is assumed that the chaotic systems under consideration are ergodic.

In view of the above, it can be said that the regime of chaotic dynamics within the bound space is understood at the level required for the problem under consideration. On the other hand, the introduction of ideas from random matrix theory to model

bound-continuum coupling with a number of independent open channels is on less secure footing.

In the Miller−Moore model, bound-continuum coupling is accounted for within the theoretical framework of an effective Hamiltonian formalism introduced mainly by Feshbach,[22] often referred to as the optical model or optical potential theory. The Hilbert space is divided into two subspaces by using orthogonal projection operators Q and P, and effective Hamiltonians for the Q and P spaces are obtained by straightforward manipulation of the Schrödinger equation.[22,23] For unimolecular reactions, an obvious perspective is that of molecular bound states and product dissociative continua.

Following the convention introduced earlier in analyses of formaldehyde data,[13] the Q and P labels are assigned to the molecular (bound) and product (continua) spaces, respectively

$$Q = \sum_i |i\rangle\langle i| \tag{2}$$

$$P = \sum \int |E'\rangle\langle E'| \tag{3}$$

The $|i\rangle$ are the bound states of the Q space, and the $|E'\rangle$ are the states of the P space. The simultaneous presence of summation and integration symbols in eq 3 indicates that continuous distributions of momentum states for relative translational motion of the products, as well as discrete product internal states, are included in the P space.

The definition of the P-space internal levels is subtle. Were the P space just the product space, these levels would be the quantum states of the products. However, to be consistent with TST, the P-space internal levels must also be defined in the region of bound-continuum coupling. For example, for a tight transition state, the transition-state frequencies are used for the P space together with free motion along the reaction coordinate. Transition-state excitations consist of quantized vibrations, each of which constitutes an independent open channel, and an associated translational continuum for each such channel. It is assumed that the system evolves from the transition state to the product space and that the statistical weights used to compute rates are those of the transition state and the molecular space. Note that, throughout this paper, the term TST is used to denote the statistical theory of unimolecular decomposition.

Following straightforward manipulations,[22,23] the Q-space effective Hamiltonian is obtained

$$H^{eff} = QHQ + QHP\frac{1}{E - PHP + i\epsilon}PHQ \tag{4}$$

It is understood that $\epsilon \to 0^+$, i.e., ϵ approaches zero as a positive quantity. Equation 4 is exact. Though H^{eff} operates only in the Q space, all interactions involving the P space are accounted for by the second term to the right of the equal sign. The operator QHP passes amplitude from the Q space to the P space. The expression $1/(E - PHP + i\epsilon)$, the resolvent of the Green's function, is equivalent to propagation in the P space. The operator PHQ passes amplitude back to the Q space.

Reaction channels are introduced by partitioning the P space into independent, i.e., noninteracting, continua

$$P = \sum_{n=1}^{K} P_n \tag{5}$$

where the index n denotes the independent continua, K is the number of such continua, and

$$P_n = \int |nE'\rangle\langle nE'| \tag{6}$$

where $|nE'\rangle$ is the ket for the nth independent continuum at energy E'. The index n accounts for the P-space internal levels summed over in eq 3. Integration can be carried out in momentum or energy space using appropriate densities of states.[24] Putting eq 5 into eq 4 yields

$$H^{eff} =$$
$$QHQ + QH\sum_{n=1}^{K}P_n\frac{1}{E - \sum_{m=1}^{K}P_m H \sum_{k=1}^{K}P_k + i\epsilon}\sum_{l=1}^{K}P_l HQ \tag{7}$$

As in eq 5, indices k, l, m, and n denote independent continua. Applying conditions of orthogonality ($P_nP_m = \delta_{nm}P_n$) and noninteraction within the P space ($P_nHP_m = \delta_{nm}P_nHP_n$) yields

$$H^{eff} = QHQ + \sum_{n=1}^{K}QHP_n\frac{1}{E - P_nHP_n + i\epsilon}P_nHQ \tag{8}$$

The corresponding Schrödinger equation

$$H^{eff}Q|\psi\rangle = EQ|\psi\rangle \tag{9}$$

yields complex energies E when the P-space eigenvalues are continuous, in which case H^{eff} is non-Hermitian. In general, eq 9 is difficult to solve, because H must be known throughout the entire bound region, as well as the region of bound-continuum coupling, whose very definition is nontrivial, particularly for barrierless unimolecular reactions. Though the presence of E in the denominator of eq 8 in general complicates the evaluation of matrix elements of H^{eff}, in the present case, the fact that the P-space eigenvalues vary continuously can be used to simplify matters, enabling eq 8 to be approximated as

$$H^{eff} = QHQ +$$
$$\sum_{n=1}^{K}\int dE'\rho_n(E')\left(QH|nE'\rangle\frac{1}{E - E' + i\epsilon}\langle nE'|HQ\right) \tag{10}$$

where $\rho_n(E')$ is the continuum density of states per unit volume of the nth channel. By assuming that $\rho_n(E')$ is independent of E' (which is appropriate for models that treat modest energy ranges) and that the bound-continuum coupling matrix elements are independent of energy, the matrix elements of H^{eff} become

$$\langle i|H^{eff}|j\rangle = \langle i|H^0|j\rangle - i\pi\sum_{n=1}^{K}\langle i|V|\phi_{nE}\rangle\langle\phi_{nE}|V|j\rangle \tag{11}$$

The density of states in eq 10 has been subsumed into $|\phi_{nE}\rangle$ and $\langle\phi_{nE}|$, each acquiring a factor of $\rho_n(E)^{1/2}$. Thus, whereas $|nE'\rangle$ is normalized by the Kronecker δ (integration over space), $|\phi_{nE}\rangle$ is normalized by the Dirac δ (integration over energy). In the above, H^0 ($=QHQ$) operates in the Q space, the matrix element $V_{in} = \langle i|V|\phi_{nE}\rangle = \langle i|H|\phi_{nE}\rangle$ represents the coupling between a bound state $|i\rangle$ and a unit energy interval of the nth channel continuum, and the $-i\pi$ factor arises from integration of the resolvent of the Green's function over the continuously varying P-space eigenvalues E'. The approximation given by eq 11 is valid for a large number of physical systems.[23] Thus, the matrix elements of H^{eff} can be expressed as

$$H^{eff}_{ij} = H^0_{ij} - i\hbar\Gamma_{ij}/2 \tag{12}$$

Effective Hamiltonian Models

J. Phys. Chem. B, Vol. 110, No. 40, 2006 **19853**

where

$$\hbar\Gamma_{ij} = 2\pi \sum_{n=1}^{K} V_{in}V_{jn} \tag{13}$$

$$= \sum_{n=1}^{K} \hbar\Gamma^{n}_{ij} \tag{14}$$

Note: V_{in} can be taken to be real without loss of generality, the matrix V_{in} is not square, and each open continuum channel introduces off-diagonal coupling among the quasi-bound states.

The $\hbar\Gamma^{n}$ in eq 14 are partial width matrices. The term partial width is used often in atomic and nuclear physics, less so in physical chemistry. For example, it is common for a collision that involves many orbital angular momenta to be assigned a partial cross section for each value of orbital angular momentum.[25] For an isolated resonance, the total width is the sum of the partial widths for the independent open channels, just as the total rate is the sum of the individual rates. In the convention used here, Γ has units of s^{-1}; the corresponding widths are obtained by multiplying Γ by $\hbar$.

The formaldehyde data that served as an impetus for the theoretical model were obtained at energies near the barrier to D_2 + CO.[2,13] Stark tuning yielded high-resolution spectra in which hundreds of resonances were observed. Many nonoverlapping resonances were recorded, and it was seen that the rates fluctuate markedly, e.g., by an order of magnitude over a 0.2 cm^{-1} interval. In this regime, the degree of resonance overlap increases with energy from mainly nonoverlapping to overlapping. As mentioned earlier, the fluctuations of rates have been attributed to chaotic dynamics of the bound region. Interference line shapes were analyzed and fitted with the model.[13]

The model emphasizes the connection between chaotic dynamics on S_0 and signatures provided by statistical fluctuations in observables in the threshold region. It was stressed that the statistical arguments are valid as long as individual resonances can be observed. This limits K in eqs 13 and 14 such that the off-diagonal matrix elements are on average smaller than the mean separation between the centers of the resonances.

II. Extension to the Regime of Overlapping Resonances

A number of authors have used eqs 12−14 in theoretical studies of unimolecular reactions in the regime of overlapping resonances.[26−37] The numerical values put into the equations have been chosen ad hoc. This does not pose a conceptual difficulty for H^0. Namely, the regime of quantum-chaotic dynamics for bound systems is understood reasonably well, and eq 1 can be used to obtain a representative set of energy levels. It has been common practice in applying eqs 12−14 to assume that H^0 is diagonal and in accord with eq 1. As mentioned earlier, bound-continuum coupling is subtler. Nonetheless, because eq 4 is rigorous, it has been assumed that the theoretical studies are on solid ground. Nuances concerning the energy dependence of eq 4 have been discussed, but the basic strategy has not been questioned.

When using eqs 12−14, the $\hbar\Gamma$ matrix is obtained by inputting matrix elements of V, indicated in eq 13, that are taken to be either random over a fixed energy interval[31,32] or drawn from a Gaussian normal distribution with zero mean, in accord with the Porter−Thomas model. The V_{in} can be taken as real with no loss of generality.

It is significant that the matrix elements of $\hbar\Gamma^{n}$ are interrelated. For a given open channel (i.e., a given value of n in eq 13), the different $\hbar\Gamma^{n}_{ij}$ consist of binary products $(V_{in}V_{jn})$ of N randomly generated matrix elements V_{in}, where N is the dimension of the H^{eff} matrix. Referring to eqs 13 and 14, for a given value of n, the matrix element $\hbar\Gamma^{n}_{ij}$ is equal to $2\pi V_{in}V_{jn}$, where the indices i and j each span the range $1 - N$. For the ith row of $\hbar\Gamma^{n}_{ij}$, the term V_{in} is constant and there are N values of the V_{jn}. Likewise for the $(i + 1)$th row, and so on. It follows that all rows are the same to within a multiplicative factor. Thus, the rank of each of the $\hbar\Gamma^{n}$ matrices is one, and each $\hbar\Gamma^{n}$ has but a single nonzero eigenvalue.

Independent open channels have been introduced by generating separate width matrices $\hbar\Gamma^{n}$ for each open channel n and summing the $\hbar\Gamma^{n}$, as indicated in eq 14. This is an energy-shell model: open channels are added to the H^{eff} matrix without introducing channel thresholds within the energy range of the matrix. (The use of an energy shell is limiting because it suppresses the $k(E)$ dependence that is a signature effect of unimolecular decomposition. This deficiency is, however, hardly the most egregious, as discussed below.) It has been assumed that the addition of width matrices whose contents are obtained independently of one another is equivalent to the inclusion of the independent open channels of TST models of unimolecular decomposition. It will be shown that this assumption is incorrect. The above model has been called the random matrix optical model. We refer to it also as the random matrix H^{eff} model.

When applying eqs 12−14 to unimolecular decomposition, it has been found that the regime of strongly overlapping resonances is characterized by a bifurcation of the distribution of widths into two groups, one of large widths and the other of small widths.[26−35] In this regime, for K open channels, the fact that the $\hbar\Gamma$ matrix is of rank K results in K large widths and $N - K$ small widths. With increasing bound-continuum coupling, the small widths get smaller and the large widths get larger.[26−35] As the system goes from nonoverlapping to strongly overlapping resonances, the rates (defined in a way that simulates time domain experiments) first saturate and then decrease as the bound-continuum coupling is increased further.[36]

The above features have one thing in common: the distributions of widths thus obtained, $P(\Gamma)$, do not behave sensibly as the bound-continuum coupling is increased. For example, they differ significantly from χ-squared distributions for K degrees of freedom, χ_K^2. The number of degrees of freedom of the χ_K^2 distribution is assumed to be equal to the number of independent open channels. In the regime where bifurcation is pronounced, the degree of overlap of the resonances is large. Nonetheless, the problem emerges as soon as the resonances begin to overlap.

Figure 3 gives an example of the regime of overlapping resonances, in which $P(\Gamma)$ differs more and more from the χ_K^2 distribution as K increases. Though the degree of overlap in Figure 3d is insufficient to result in a bifurcation for the given set of parameters, the deviation from a χ_K^2 distribution is inconsistent with TST. A bifurcation can always be brought about by increasing K (and concomitantly N, with $N \gg K$) or by increasing the bound-continuum coupling per channel, as shown in Figure 4. Though the latter violates the 2π rule (Appendix A) it has been used by numerous authors.[26−37]

The theoretical results obtained by using eq 12 are inconsistent with what is known about unimolecular decomposition. There exist numerous data on the unimolecular decomposition of polyatomic molecules. These indicate that distributions of rate coefficients do not bifurcate in the regime of strongly overlapping resonances, where nearly all such reactions occur. The rate coefficients $k(E)$ increase monotonically with E. If anything, the variation is boring. A bifurcation of the kind reported in the theoretical studies would be seen in time-resolved

19854 *J. Phys. Chem. B, Vol. 110, No. 40, 2006*

Wittig and Bezel
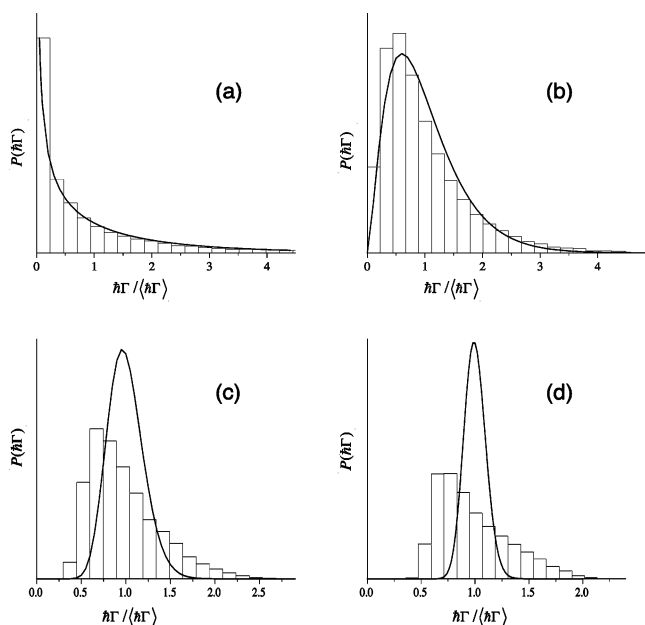
Figure 3. Numerical experiments using eqs 12–14, showing distributions of the widths upon diagonalization. The matrices are of dimension 2000 with Wigner-spaced diagonals having $\rho = 1$. The V_{in} are drawn from a Gaussian normal distribution with zero mean; they satisfy the 2π rule: $\langle \Gamma^n \rangle = 1/h\rho$. The $P(\hbar\Gamma)$ are the distributions of widths obtained by diagonalizing eq 12; entries (a–d) are for $K = 1, 5, 50,$ and 200, respectively. To avoid edge effects from the matrix boundaries, only states with $-500 \le E \le 500$ have been used in the histograms. All results have been averaged over 10 matrices. The smooth curves are the χ-squared distributions χ_K^2.
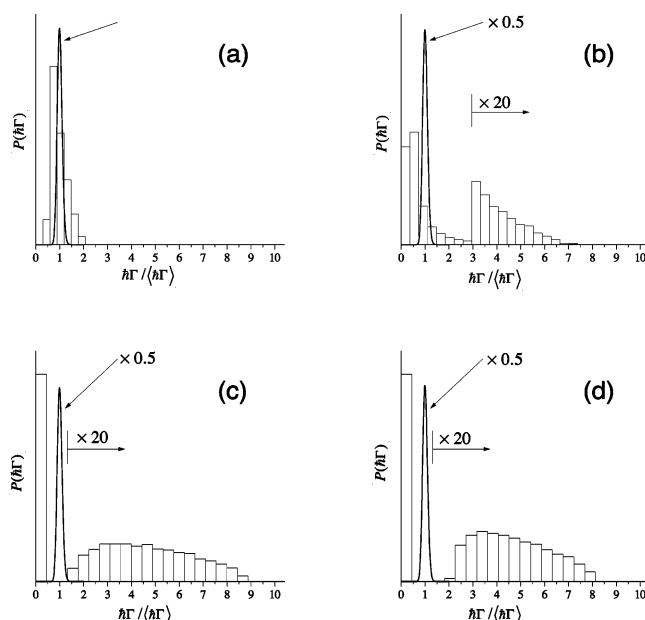
Figure 4. Examples of bifurcations. The initial matrices are the same as those used in Figure 3d, except imaginary parts have been multiplied by 1, 3, 10, and 100 prior to diagonalization, for (a–d), respectively. The smooth curves are the χ-squared distributions χ_K^2.

experiments in which reaction products are detected. Signals would display both rapid rise times and much slower rise times. There would be no way to fit the data to a smooth $k(E)$.

In rare cases, structure in $k(E)$ versus E has been observed at energies not too far above the reaction threshold,[38,39] and rates fluctuate with small changes in E when accessing a modest number of open channels. Also, a few special cases, such as HFCO[39] and HOCl,[40,41] are nonstatistical due to incomplete

intramolecular vibrational redistribution, and subtleties have been uncovered in other systems. However, as a general statement, it is safe to say that there are no bifurcations. Thus, applying eqs 12–14 to unimolecular decomposition will not yield correct results.

III. Source of the Problem

Equations 12–14 should not be used in TST models of unimolecular decomposition. Equation 12, with H^0 diagonal, represents a system of zero-order resonances (i.e., the diagonal matrix elements) that interact with one another via the continua as per the off-diagonal matrix elements of $-i\hbar\Gamma/2$. This mathematical structure stands in the way of satisfying the requirement that the system evolves to products via TS levels that are accessed independently. Open channels modeled as $-i\hbar\Gamma^n/2$ matrices, though satisfying many statistical criteria, are inconsistent with TST.

In the regime of nonoverlapping resonances, matrix representations of H^{eff} have correct physics inputted on the diagonal, and the off-diagonal matrix elements are too small to produce significant effects. Thus, to a good degree of accuracy, a system initially in the Q space decays irreversibly to the P space, in accord with TST. For example, see Figure 3a.

In the regime of strongly overlapping resonances, the average magnitude of the off-diagonal matrix elements is well in excess of the average energy separation between the centers of the resonances. In this case, the off-diagonal matrix elements of $\hbar\Gamma$ are responsible for results that contradict experiment. Strong couplings that occur via the continua are appropriate for systems such as adiabatic PESs coupled by strong nonadiabatic interactions. However, such couplings have no place in models of unimolecular decay. Here, the TS levels for the independent open channels, once reached, evolve to products. There is some reflected flux, making the transmission coefficient through the TS region less than unity, but nothing justifies the strong couplings between zero-order resonances, via the continua, that appear in the H^{eff} matrix.

In TST, each open channel contributes $1/h\rho$ to the rate, where ρ is the density of participating states. The rate for K open channels is given by $K/h\rho$. In the random matrix H^{eff} model, independent continua (indices n in eqs 13 and 14) are introduced by summing $-i\hbar\Gamma^n/2$ matrices, with the average value of the diagonal elements obeying $\langle \Gamma_{jj}^n \rangle = 1/h\rho$, i.e., enforcing the 2π rule. Thus, when summing over the open channels, the diagonal elements yield $\langle \Gamma_{jj} \rangle = K/h\rho$, in accord with TST. Moreover, the diagonal elements of the width matrix follow a χ_K^2 distribution.

Bifurcation of the distribution of widths upon diagonalization makes it difficult to define an experimentally observable rate. The average rate is preserved (trace conservation), and it is not feasible that only one or the other of the groups corresponds to unimolecular decomposition. Peskin et al., using a sensible definition of the experimentally observable rate, fitted temporal decays of initial Q-space wave packets to exponentials,[36] while avoiding the regime of pronounced bifurcation.

When the rate calculated by using the above procedure saturates with a sufficiently large number of open channels, i.e., $\partial k/\partial K = 0$, which has been verified by numerous authors,[26–37] the system is manifestly at odds with TST. In fact, it has been shown that this rate decreases with the addition of further open channels, and no amount of ad hoc adjustment can remedy the problem.

The 2π rule states that the average separation between adjacent resonances (i.e., ρ^{-1}) divided by the average resonance

width is equal to 2π; see Appendix A. This indicates that for each open channel the partial widths are, for the most part, isolated. We say "for the most part" because a ratio of 2π inevitably accommodates a small degree of overlap. An isolated partial width is equal to the corresponding single-channel reaction rate times $\hbar$. Thus, with the 2π rule enforced, the regime of overlapping resonances in unimolecular decomposition is seen to be the consequence of many channels being open.

When partial widths for the same open channel overlap, interference occurs, for example, in an absorption or Stark-tuning spectrum. Such interferences have been observed (using Stark tuning spectroscopy) and analyzed by Polik et al.[13] There will always be some degree of interference for a given open channel, but this will be modest. Thus, the partial widths can be said to be mainly isolated. Interference is also possible if a product species is monitored in one of its rovibronic levels, e.g., by recording a yield spectrum. When two or more open channels yield the monitored state (plus a specific state of the other fragment), these constitute separate pathways to the same products. Thus, interference effects have been reported over a broad energy range.[42,43]

Because TST open channels are independent and the partial widths for a given open channel are mainly isolated, the total widths can be obtained by summing partial widths. The resonances overlap in the sense that their average width exceeds the average spacing. However, this differs qualitatively from cases in which resonances interact strongly via a common continuum. Thus, in modeling unimolecular decomposition, there should be no complication with many open channels. In the regime of strongly overlapping resonances, fluctuations should be diminished markedly relative to the threshold region, and $k(E)$ should approach $K\langle\Gamma^n\rangle = K/h\rho$. If this goes awry in the regime of strongly overlapping resonances, the model is at fault.

Equation 4 is exact, and eq 12, being a good approximation to eq 4, yields accurate results—but if not for unimolecular decomposition, then for what physical system? It is the *interpretation* of the Q space as the molecular space and the P space as the product space that breaks down with increasing bound-continuum coupling. It will be shown below how strong bound-continuum coupling causes certain states to acquire properties of the continua. This decouples them from the molecular region, causing the aforementioned bifurcation.

IV. What Does the Random Matrix Optical Model Represent?

Equations 12–14 with the V_{in} in eq 13 chosen randomly have been used to construct abstract mathematical models of unimolecular decomposition. In attempting to bring such models into registry with TST, it has been tacitly assumed that the TS levels are dissolved into the Q and/or P spaces, thereby providing bound-continuum coupling.

Insight can be obtained by solving the model shown in Figure 5. The ϕ_s are coupled to a continuum via ϕ_n, which acts as a gateway between the ϕ_s manifold and the continuum. It is assumed that the $V_{nE'}$ are independent of energy. This system cannot serve as a model of unimolecular decomposition: (*i*) ϕ_n does not approximate an open channel, because it has fixed energy; (*ii*) there is no way to consistently define channel thresholds, because widths are distributed smoothly in energy; and (*iii*) the widths (locally averaged to remove random fluctuations) depend on their distance from E_n.

We now examine exact solutions of this model for a range of coupling strengths. A bifurcation of the distribution of widths
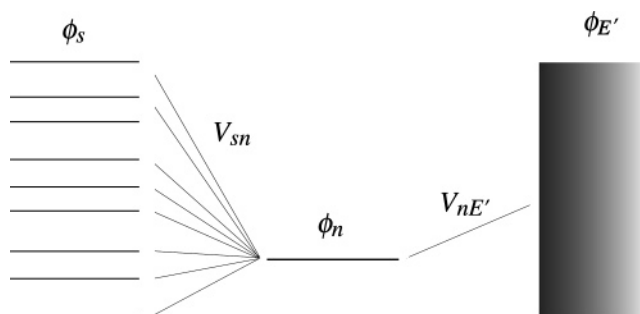
Figure 5. A manifold of bound levels ϕ_s, which have nearest-neighbor spacings given by eq 1, is coupled via ϕ_n (whose energy is E_n) to a continuum $\phi_{E'}$. The V_{sn} matrix elements that couple ϕ_n to the manifold of ϕ_s levels assume different values for the different ϕ_s levels. The $V_{nE'}$ matrix elements are assumed to be independent of energy.

will be identified for large bound-continuum coupling. Expressing this model as an effective Hamiltonian and carrying out a change of basis reveals a form that satisfies eq 13. Restricting the energy range to a shell near the center energy E_n yields the random matrix H^{eff} model version of eq 12, thus identifying its content for the case of a single gateway state. Extension to multiple gateway states is straightforward.

Exact Solution. The model in Figure 5 is solved exactly by extending the method of integration residuals introduced by Fano for analyses of interference line shapes (Appendix B).[44] When coupling of ϕ_n to the continuum is weak relative to coupling of ϕ_n to the ϕ_s, the resonances are sharp, as shown in Figure 6a. Because the solution is exact, the eigenfunctions $\psi(E)$ reveal how ϕ_n and ϕ_s are distributed in energy. For example, a single resonance can be resolved into how its ϕ_s and ϕ_n constituents are distributed. This is shown in Figure 6 in plots of $|\langle\psi(E)|\phi_n\rangle|^2$ versus E. Note that this differs from the H^{eff} approach, which yields widths of resonances and their compositions in terms of basis vectors but provides no information about dynamical processes in the continuum.

In going from (a) to (d) in Figure 6, $|V_{nE'}|$ increases, with the other parameters constant. This brings about interesting changes. Near E_n, the resonance widths at first increase. However, as the coupling of ϕ_n to the continuum continues to increase, there comes a point where these widths begin to decrease. This occurs because ϕ_n is being distributed throughout the continuum over an increasingly broad energy range. At energies well-removed from E_n, resonance widths increase with bound-continuum coupling, whereas resonance widths near E_n decrease. For a given value of $V_{nE'}$, the largest widths are located near E_n, subject to the randomness of the V_{sn}.

Increasing the coupling of ϕ_n to the continuum (with fixed V'_{sn}) uncouples ϕ_n from the ϕ_s and dissolves it into the continuum. Thus, increasing coupling to the continuum causes one width (i.e., that of ϕ_n) to increase while the others decrease. This is a bifurcation of the distribution of widths.

Solutions to the model shown in Figure 5 are interpreted straightforwardly because the role of ϕ_n is known from the outset. For example, the bifurcation in Figure 6d is unambiguous. The model shown in Figure 5 can also be converted to a form that highlights its relationship to eq 13. It is shown below that eqs 12 and 13 applied to the case of a single open channel represent the model shown in Figure 5.

H^{eff} Matrix Representation of the Model Problem. The model shown in Figure 5 has the simple H^{eff} matrix representation shown in Figure 7. The energies of the ϕ_s and ϕ_n levels lie on the diagonal, and the off-diagonal matrix elements V'_{sn} are drawn randomly from a Gaussian normal distribution with zero
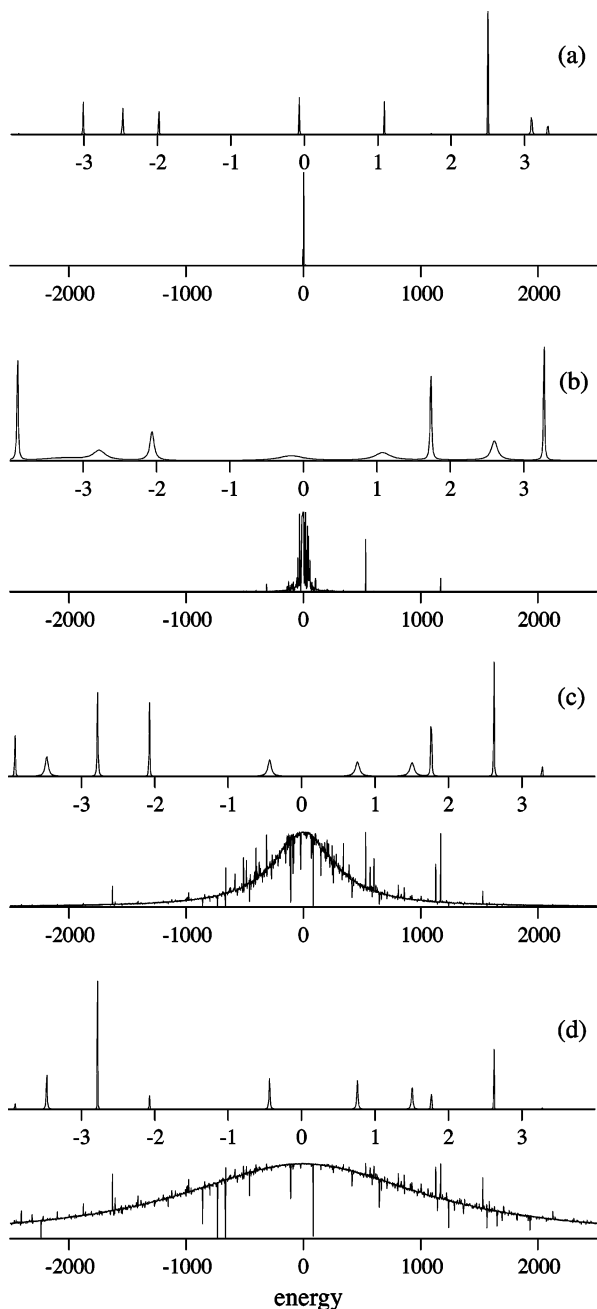
Figure 6. Exact solutions of the model problem presented in Figure 5 with 5000 bound states and $\rho = 1$. The V_{sn} were drawn from a Gaussian normal distribution having zero mean and dispersion of 2. Panels (a–d) are for $V_{nE'}$ values of 0.2, 2.5, 10, and 20, respectively. The upper plots for each of the panels are the sums of the $|\langle \psi(E)|\phi_s\rangle|^2$ for a modest energy interval centered at E_n; the lower plots are $|\langle \psi(E)|\phi_n\rangle|^2$. With the latter, low resolution shows the overall envelope, while at high resolution, $|\langle \psi(E)|\phi_n\rangle|^2$ varies markedly near each of the resonances. Note the different horizontal scales for the upper and lower plots. In (a), ϕ_n and the ϕ_s are mixed strongly within the energy range of their interaction, which is given by $2\pi\langle|V_{sn}|^2\rangle\rho$, and the decay width of ϕ_n is shared among the mixed levels. In (c) and (d), ϕ_n is uncoupled from the ϕ_s, and the resonance positions in the upper plots are essentially those of the ϕ_s (ϕ_n cannot be seen in the upper plots); these resonance widths decrease with increasing $V_{nE'}$.

mean. Primes are used to label the H^{eff} matrix before the change of basis. The only imaginary term is $-i\hbar\Gamma'_{nn}/2$

$$-i\hbar\Gamma'_{ij}/2 = -i\hbar\gamma/2\,\delta_{in}\delta_{nj} \qquad (15)$$

where γ is the decay rate of the ϕ_n level, and δ_{in} and δ_{nj} are Kronecker δ's.
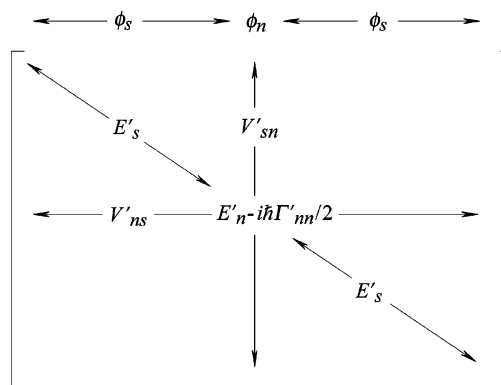
Figure 7. The ϕ_s energies are E'_s. The complex energy of ϕ_n is $E'_n - i\hbar\Gamma'_{nn}/2$. The matrix elements V'_{sn} couple ϕ_n and ϕ_s.

The goal is to transform the $H' - i\hbar\Gamma'/2$ matrix into the form of eq 13. To achieve this, the matrix is subjected to a change of basis that mixes ϕ_n and the ϕ_s, with the $-i\hbar\Gamma'_{nn}/2$ term ignored. Namely, the H' part is diagonalized. In leaving aside the decay of ϕ_n to the continuum, ϕ_n is treated as a member of the quantum-chaotic bound states. The similarity transformation that diagonalizes H' is then applied to $H' - i\hbar\Gamma'/2$. As a result, terms appear in both the diagonal and off-diagonal positions of the new width matrix, $\hbar\Gamma$.

It is now shown that $\hbar\Gamma$ satisfies eqs 12 and 13. The matrix elements of $\hbar\Gamma$ are given by

$$\hbar\Gamma_{ij} = \sum_{k,q} S_{ik}\hbar\Gamma'_{kq}(S^{-1})_{qj} \qquad (16)$$

$$= \sum_{k,q} S_{ik}\hbar\Gamma'_{kq}S_{jq} \qquad (17)$$

where S is the matrix that diagonalizes H', and $S^{-1} = S^T$ (transpose) has been used. Because the $\hbar\Gamma'$ matrix has but the single nonzero element given by eq 15, eq 17 becomes

$$\hbar\Gamma_{ij} = \sum_{k,q} S_{ik}\hbar\gamma\delta_{kn}\delta_{nq}S_{jq} \qquad (18)$$

$$= \hbar\gamma S_{in}S_{jn} \qquad (19)$$

Thus, equating the expressions for $\hbar\Gamma_{ij}$ given by eqs 13 and 19, the elements of the nth column of S (i.e., the S_{in} in eq 19) are equal to $(2\pi/\hbar\gamma)^{1/2}$ times the V_{in} in eq 13. Referring to Figure 7, in diagonalizing H', ϕ_n–ϕ_s coupling yields states whose expansion coefficients are random. Thus, the chaotic nature of the intramolecular dynamics has resulted in coefficients S_{in} that have the same statistical properties as the V_{in} in eq 13. Thus, the equivalence of the model shown in Figure 5 and the random matrix H^{eff} model is proven.

To illustrate with an example the statistical properties of the S_{in}, a modest energy interval near the center energy E_n, have been analyzed, as indicated in Figure 8a. Figure 8b shows that the randomness of the V'_{sn} matrix elements, whose distribution is Gaussian, has been transferred to the S_{in}, which are seen to also exhibit a Gaussian distribution.

Interpretation. The model depicted in Figure 5 of a single gateway state ϕ_n that couples the ϕ_s levels to a continuum has been cast in a form that invites comparisons to eqs 12 and 13 in the regime of overlapping resonances. Increasing the value of γ in eq 19 causes a bifurcation of the distribution of widths and brings about strong resonance overlap that is evident in the diagonal matrix elements of $H^0 - i\hbar\Gamma/2$.

Effective Hamiltonian Models
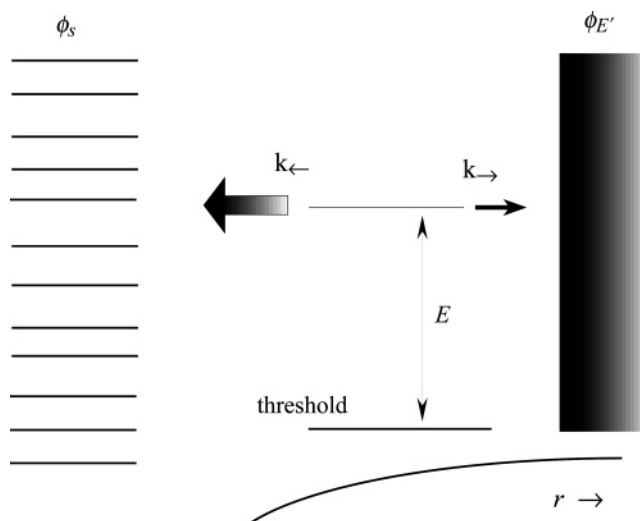
J. Phys. Chem. B, Vol. 110, No. 40, 2006 **19857**
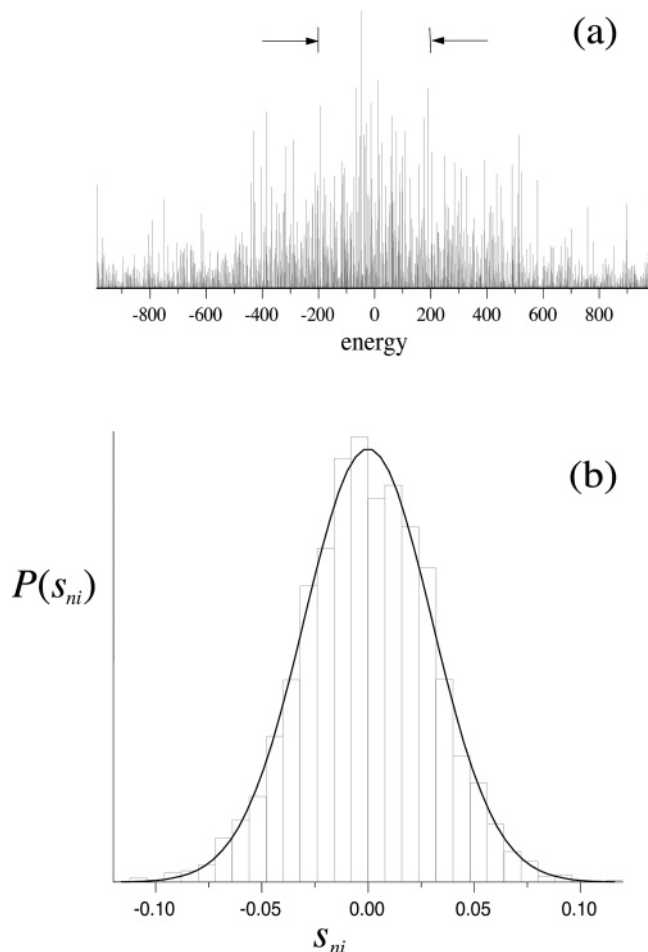
Figure 8. (a) Stick spectrum for a single ϕ_n coupled to 2000 ϕ_s. The V_{sn} matrix elements were drawn from a Gaussian normal distribution with zero mean and dispersion = 10, analogous to Figure 6c. (b) s_{ni} distribution: arrows indicate the energy region chosen for analysis. The solid line indicates a Gaussian distribution. Results are averaged over 10 matrices.

Figure 9. The ϕ_s are zero-order bound states, and $\phi_{E'}$ is a continuum. The lowest TS level is indicated as the threshold for the barrierless pathway shown. The energy available for reaction coordinate translational motion in the TS region is labeled E.

Additional gateway states ϕ_m can be introduced that are coupled to their respective continua $\phi_{mE'}$ as well as to the manifold of ϕ_s levels. For example, additional terms $-i\hbar\Gamma'_{mm'}/2$ and V'_{sm} could be added to the matrix shown in Figure 7. Diagonalization of the real part again yields a nondiagonal width matrix. This matrix is the superposition of the partial width matrices associated with the different values of m. The randomness of the V'_{sm} matrix elements is transferred to the partial width matrices.

The partial width matrices obey eq 13. In this sense, they are independent of one another. However, the gateway states, together with their respective continua, are automatically coupled to one another via the ϕ_s levels. This is true regardless of the details of the model. It is a consequence of the fact that coupling of the ϕ_s to the continua is via bound states. The partial width matrices are not independent in the sense of TST models of unimolecular decomposition, in which the continua are not coupled to one another.

The above example explains the "trapping effect" discussed previously,[26−35] in which the magnitudes of the imaginary parts of the eigenvalues of the $N - K$ trapped states first saturate and then decrease with increasing coupling to the continuum. In these studies, the $N - K$ levels have sometimes been assigned to RRKM-type behavior, e.g., for a restricted range of bound-continuum coupling strengths. However, the results presented above show that such a model does not represent unimolecular

decomposition, regardless of the degree of coupling to the continua. To have independent open channels that are consistent with TST, a model is needed that has one-way fluxes to the continua via the corresponding TS levels.

V. A Simple Model

The flaws of the random matrix H^{eff} model are lethal, and there is no remedy. Thus, an alternate model is introduced. Figure 9 indicates one possibility. The salient features are outlined here; a complete description will be published later. This model accounts for fluctuation phenomena, and it has no χ_K^2 or bifurcation problems.

Recall that, for each open channel, the ratio of the average separation between resonances to the average resonance width is 2π. This can also be stated in terms of the decay rates of the TS region to the bound space and to the continuum, i.e., the ratio of the former ($k_\leftarrow$) to the latter ($k_\rightarrow$) is equal to 2π. As E increases, $k_\rightarrow$ increases, and consequently, the coupling of the TS region to the bound region must increase in order to maintain the average resonance decay rate equal to $1/h\rho$.

The Wigner distribution provides bound-state energies for a system whose classical dynamics are chaotic. These can be taken as the centers of the resonances. Because of the nonoverlapping nature of the resonances belonging to a single open channel and the independence of the open channels, couplings to the channel continua do not shift significantly the centers of the resonances. The average single-channel resonance decay rate $\langle\Gamma^n\rangle$ is equal to $1/h\rho$, and the statistical fluctuations of the single-channel decay rates from one resonance to the next follow a χ-squared distribution with one degree of freedom.

Because the relevant physics is inputted directly, there is no computation. For a single open channel, the resonance center energies follow a Wigner distribution, and the partial widths fluctuate about the value $1/2\pi\rho$. Multiple open channels are introduced by adding partial widths for each resonance, starting at each channel threshold, with the partial widths for each open channel obtained independently. The result is that (i) the rate increases, on average, in steps of $1/h\rho$; (ii) the degree of resonance overlap increases with E; and (iii) fluctuations in $k(E)$ decrease with E according to the averaging that results from the successive openings of channels. The introduction of channel

thresholds differs from the random matrix H^{eff} model, which is an energy-shell model that, by definition, has no channel thresholds.

The statistical theory of unimolecular decomposition is based on the assumption that each open channel is independent and is accessed via a TS level. Though the TS levels are not explicit in this model, the 2π rule imposes constraints. For example, as E increases, the rate with which the TS region evolves to its continuum ($k_\rightarrow$) increases. The corresponding increase in $k_\leftarrow$ requires that the TS lies at smaller r. In simple terms, the TS region, by definition, lies between regions of chaotic and regular dynamics. The more vigorously the system moves toward the regular region, the more strongly it must be coupled to the chaotic region in this balancing act. This stronger coupling can only occur closer to the molecular region. Such "tightening of the TS" is an established phenomenon.[5,6] This effect holds for each open channel. Because the channels are independent, so are their TS properties. For example, when more than one channel is open, each of the TS levels for the different channels lies at a different location along the reaction coordinate. The change in TS location with E is most pronounced for barrierless reactions just above the channel thresholds.

VI. Summary

Effective Hamiltonian models have been used previously to model unimolecular decomposition with emphasis on quantum fluctuation phenomena and bifurcations of the distribution of widths. Specifically, with the Hilbert space partitioned into Q and P subspaces, H^{eff} is approximated as $H^0 - i\hbar\Gamma/2$. This random matrix H^{eff} model fails in the regime of overlapping resonances, where most unimolecular reactions occur.

In this paper, it has been shown that dividing the Hilbert space into two subspaces, though mathematically exact, stymies satisfying the requirements of a statistical theory of unimolecular decomposition. Furthermore, it has been shown that all implementations to date of $H^{eff} = H^0 - i\hbar\Gamma/2$ are models in which gateway states couple a manifold of bound levels to continua. Bound-continuum coupling via gateways states is incompatible with independent open channels. Therefore, such models cannot represent unimolecular decomposition in the regime of overlapping resonances. A simple model has been pointed out that accounts for quantum fluctuations without the aforementioned problems.

Appendix A. The 2π Rule

A useful tool for dealing with the regime of overlapping resonances in unimolecular decomposition is the 2π rule. To show how this works, a simple calculation is used to obtain the rate per independent open channel for a microcanonical system in the statistical limit. Figure 10 shows a two-dimensional section of the multidimensional phase space, where x is the reaction coordinate and p_x is its conjugate momentum. Dynamical processes in the molecular region are assumed to be chaotic, as indicated by the irregular trajectory, while in the product region, they are regular. It is assumed that the chaotic dynamics are fast in comparison to dissociation and that they are ergodic, i.e., the phase space is filled uniformly by trajectories. It is also assumed that the system exits the chaotic region via a region of the phase space that separates the chaotic and regular regions along the reaction coordinate, i.e., the TS region indicated by
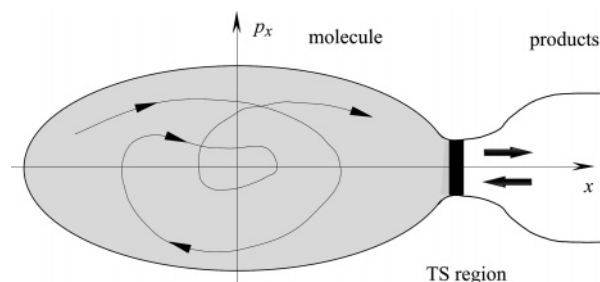
Figure 10. Multidimensional classical motion projected onto the $x - p_x$ plane. The shaded area and the curves extending into the product region represent the accessible phase space at energy E. The TS region separates the molecular and product regions. Trajectories move from left to right in the upper half-plane and from right to left in the lower half-plane. Dissociation occurs for positive p_x.

the black area in the figure. From the TS, the system is assumed to proceed to products.

The TS introduced above is for a single open channel. Consider now the channel having the lowest threshold. The subsystem consisting of the $z - 1$ degrees of freedom orthogonal to the reaction coordinate at the TS, where z is the total number of degrees of freedom, is in its lowest energy level. At the TS, all of the available energy is in one-dimensional translational motion along the reaction coordinate.

The phase volumes are calculated for a small energy interval, ΔE. The phase volumes of the TS (i.e., ΔV_{TS}) and of the chaotic region (i.e., ΔV) are given, respectively, by

$$\Delta V_{TS} = h^{z-1} \int_{TS} dx \Delta p_x \tag{A1}$$

$$\Delta V = h^z \rho \Delta E \tag{A2}$$

where integration is carried out over the TS region and ρ is the density of states. The phase volume of a single z-dimensional state is h^z. Thus, the single-channel microcanonical rate coefficient $k^{(1)}$ is given by

$$k^{(1)} = \frac{\Delta V_{TS}}{\Delta V} \frac{1}{\tau_{TS}} \tag{A3}$$

where $\Delta V_{TS}/\Delta V$ is the probability that the system is in the TS region and τ_{TS} is the transit time through the TS region. Putting eqs A1 and A2 into eq A3 yields

$$k^{(1)} = \frac{1}{h\rho} \frac{1}{\tau_{TS}} \int_{TS} dx \frac{\Delta p_x}{\Delta E} \tag{A4}$$

Using the fact that $\Delta E = v\Delta p_x$, where $v = dx/dt$, in the TS region yields

$$k^{(1)} = \frac{1}{h\rho} \frac{1}{\tau_{TS}} \int_{TS} \frac{dx}{v} \tag{A5}$$

$$= \frac{1}{h\rho} \frac{1}{\tau_{TS}} \int_{TS} dt \tag{A6}$$

Because the integral is, by definition, equal to τ_{TS}, eq A6 becomes

$$k^{(1)} = \frac{1}{h\rho} \tag{A7}$$

Thus, the rate coefficient for the lowest open channel is equal to $1/h\rho$, independent of E.

Effective Hamiltonian Models

J. Phys. Chem. B, Vol. 110, No. 40, 2006 **19859**

The system consisting of $z - 1$ degrees of freedom orthogonal to the reaction coordinate has excited TS levels that constitute independent open channels. Each follows the prescription given by eqs A1−A7 and contributes $1/h\rho$ to the overall rate. Each has a TS that is accessed without bias from the chaotic region. This is why the channels are said to be independent. Thus, the expression for the microcanonical rate coefficient is given by $k(E) = K/h\rho$, where K is the number of independent open channels.

The single-channel rate coefficient $k^{(1)} = 1/h\rho$ corresponds to the average single-channel resonance decay rate $\langle \Gamma^n \rangle$ where n denotes a generic open channel. The individual single-channel decay rates Γ_i^n correspond to partial widths $\hbar\Gamma_i^n$, where the subscript denotes specific resonances. This relationship can be used because, for a given independent open channel, the widths are mainly nonoverlapping, as seen from the expression

$$\frac{\text{average separation between resonances}}{\text{average resonance width per open channel}} = \frac{\rho^{-1}}{\langle \hbar\Gamma^n \rangle} \quad \text{(A8)}$$

$$= 2\pi \quad \text{(A9)}$$

where $\langle \Gamma^n \rangle = 1/h\rho$ has been used. This constitutes the 2π rule. It shows that the resonances for a single independent open channel have modest overlap.

Appendix B. Exact Solution of the Model Problem

Referring to the model problem shown in Figure 5, the eigenfunctions $\psi(E)$ are expanded in the basis of bound (ϕ_n and ϕ_{s_j}) and continuum ($\phi_{E''}$) functions

$$\psi(E) = C_n\phi_n + \sum_{s_j} C_{s_j}\phi_{s_j} + \int dE'' C_{E''}\phi_{E''} \quad \text{(B1)}$$

The coefficients are $C_n = \langle\phi_n|\psi(E)\rangle$, $C_{s_j} = \langle\phi_{s_j}|\psi(E)\rangle$, and $C_{E''} = \langle\phi_{E''}|\psi(E)\rangle$. The $\phi_{E''}$ are normalized according to $\langle\phi_{E'}|\phi_{E''}\rangle = \delta(E' - E'')$. To obtain equations for the coefficients, the Schrödinger equation, $(H_0 + V)\psi(E) = E\psi(E)$, is applied to eq B1, yielding

$$E\psi(E) = C_n(E_n + V)\phi_n + \sum_{s_j} C_{s_j}(E_{s_j} + V)\phi_{s_j} +$$
$$\int dE C''_{E''}(E'' + V)\phi_{E''} \quad \text{(B2)}$$

where E_n, E_{s_j}, and E'' are eigenvalues of H_0. Projecting eq B2 onto $\langle\phi_{s_i}|$, $\langle\phi_{E'}|$, and $\langle\phi_n|$ yields, respectively

$$(E - E_{s_i})C_{s_i} = V_{s_in}C_n \quad \text{(B3)}$$

$$(E - E')C_{E'} = V_{E'n}C_n \quad \text{(B4)}$$

$$(E - E_n)C_n = \sum_{s_j} V_{ns_j}C_{s_j} + \int dE'' V_{nE''}C_{E''} \quad \text{(B5)}$$

where $V_{s_in} = \langle\phi_{s_i}|V|\phi_n\rangle$, $V_{E'n} = \langle\phi_{E'}|V|\phi_n\rangle$, and $V_{nE''} = \langle\phi_n|V|\phi_{E''}\rangle$. Referring to Figure 5, V has no nonzero off-diagonal matrix elements among the ϕ_{s_j} bound states or among the $\phi_{E''}$ continuum states. Equation B3 can be inverted to yield C_{s_i} as long as $E \neq E_{s_i}$. Because the E_{s_i} values are discrete, this poses no difficulty; $E \neq E_{s_i}$ can always be chosen when evaluating $\psi(E)$. Thus, eq B3 becomes

$$C_{s_i} = \frac{1}{E - E_{s_i}} V_{s_in}C_n \quad \text{(B6)}$$

where it is understood that $E \neq E_{s_i}$. Inverting eq B4 requires more care because E' varies continuously. Though $E' = E$ is certain to occur, eq B4 can be inverted as long as (i) E' is not allowed to be equal to E when $E - E'$ appears in the denominator, and (ii) a term is added that is present only at $E' = E$ and satisfies $(E - E') C_{E'} = 0$. This "residual" term is proportional to $\delta(E - E')$, and it can be a function of E. Because we are dealing with the full Hamiltonian rather than an effective Hamiltonian, this integration residual $z(E)$ must be real. Thus, the inversion of eq B4 can be written

$$C_{E'} = V_{En}C_n\left[\frac{1}{E - E'} + z(E)\delta(E - E')\right] \quad \text{(B7)}$$

The first term in brackets is taken as the principal part upon integration, and it is assumed that $V_{E'n}$ in eq B4 is constant (V_{En}) for all E'. Thus, the equations for the coefficients become

$$C_{s_i} = C_n V_{s_in} \frac{1}{E - E_{s_i}} \quad \text{(B8)}$$

$$C_{E'} = C_n V_{En}\left[\frac{1}{E - E'} + z(E)\delta(E - E')\right] \quad \text{(B9)}$$

$$C_n(E - E_n) = \sum_{s_j} C_{s_j} V_{ns_j} + V_{nE} \int dE'' C_{E''} \quad \text{(B10)}$$

Together with the normalization of $\psi(E)$, eqs B8−B10 describe fully the system shown in Figure 5. Substituting eqs B8 and B9 into eq B10 yields an expression for $z(E)$

$$z(E)|V_{En}|^2 = E - E_n - \sum_{s_j} \frac{|V_{ns_j}|^2}{E - E_{s_j}} - \int dE' \frac{|V_{En}|^2}{E - E'} \quad \text{(B11)}$$

where it is understood that the principal part is taken upon integration. Thus, for a given set of parameters (E_n, E_{s_i}, V_{En}, V_{s_in}), $z(E)$ is obtained. Because V_{nE} is assumed to be independent of E, the principal part integral in eq B11 vanishes, leaving

$$z(E)|V_{En}|^2 = E - E_n - \sum_{s_j} \frac{|V_{ns_j}|^2}{E - E_{s_j}} \quad \text{(B12)}$$

Applying the normalization condition $\langle\psi(E)|\psi(\bar{E})\rangle = \delta(E - \bar{E})$ yields C_n;[44] the coefficients C_{s_i} and $C_{E'}$ are then obtained by using eqs B8 and B9. With the phase set equal to zero, C_n is given by

$$C_n = \frac{1}{|V_{En}|} \frac{1}{\sqrt{\pi^2 + z^2}} \quad \text{(B13)}$$

where both π^2 and z^2 arise as integration residuals,[44] and eq B8 yields

$$C_{s_i} = \frac{V_{s_in}}{|V_{En}|} \frac{1}{E - E_{s_i}} \frac{1}{\sqrt{\pi^2 + z^2}} \quad \text{(B14)}$$

To summarize, for a given value of E, $z(E)$ is evaluated by using eq B12. The expansion coefficients are then obtained by using eqs B13, B14, and B9. The solution is exact. Because the $\psi(E)$ belong to a continuum, they are not square integrable.

Instead, $\langle\psi(\bar{E})|\psi(E)\rangle = \delta(E - \bar{E})$. It is easy to take a large enough number of $\psi(E)$ so that $|\langle\phi_{s_i}|\psi(E)\rangle|^2$ versus E appears continuous.

References and Notes

(1) Miller, W. H.; Hernandez, R.; Moore, C. B.; Polik, W. F. *J. Chem. Phys.* **1990**, *93*, 5657.

(2) Polik, W. F.; Guyer, D. R.; Miller, W. H.; Moore, C. B. *J. Chem. Phys.* **1990**, *92*, 3471.

(3) Hernandez, R.; Miller, W. H.; Moore, C. B.; Polik, W. F. *J. Chem. Phys.* **1993**, *99*, 950.

(4) Baer, T.; Hase, W. L. *Unimolecular Reaction Dynamics*; Oxford University Press: New York, 1996.

(5) Gilbert, R. G.; Smith, S. C. *Theory of Unimolecular and Recombination Reactions*; Blackwell: Oxford, 1990.

(6) Mies, F. H.; Krauss, M. *J. Chem. Phys.* **1966**, *45*, 4455.

(7) Mehta, M. L. *Random Matrices*, 2nd ed.; Academic Press: New York, 1991.

(8) Brody, T. A.; Flores, J.; French, J. B.; Mello, P. A.; Pandey, A.; Wong, S. M. M. *Rev. Mod. Phys.* **1981**, *53*, 385.

(9) Porter, C. E.; Thomas, R. G. *Phys. Rev.* **1956**, *104*, 483.

(10) Porter, C. E. *Statistical Theories of Spectra: Fluctuations*; Academic Press: New York, 1965.

(11) Hughes, D. J.; Harvey, J. A. *Phys. Rev.* **1955**, *99*, 1032.

(12) Nadler, I.; Noble, M.; Reisler, H.; Wittig, C. *J. Chem. Phys.* **1985**, *82*, 2608.

(13) Polik, W. F.; Guyer, D. R.; Moore, C. B. *J. Chem. Phys.* **1990**, *92*, 3453.

(14) Guyer, D. R.; Polik, W. F.; Moore, C. B. *J. Chem. Phys.* **1986**, *84*, 6519.

(15) Polik, W. F.; Moore, C. B.; Miller, W. H. *J. Chem. Phys.* **1988**, *89*, 3584.

(16) Weisshaar, J. C.; Moore, C. B. *J. Chem. Phys.* **1988**, *70*, 5135.

(17) Wigner, E. P. *Ann. Math.* **1955**, *62*, 548.

(18) Wigner, E. P. *Ann. Math.* **1957**, *65*, 203.

(19) Wigner, E. P. *Canadian Mathematical Congress Proceedings*; University of Toronto Press: Toronto, 1957.

(20) Dyson, F. J. *J. Math. Phys.* **1962**, *3*, 166.

(21) Dyson, F. J.; Mehta, M. L. *J. Math. Phys.* **1963**, *4*, 701.

(22) Feshbach, H. *Theoretical Nuclear Physics*; Wiley: New York, 1992.

(23) Cohen-Tannoudji, C.; Dupont-Roc, J.; Grynberg, G. *Atom-Photon Interactions*; Wiley: New York, 1992.

(24) Rodberg, L. S.; Thaler, R. M. *Introduction to the Quantum Theory of Scattering*; Academic Press: New York, 1967.

(25) Pauly, H. In *Atom-Molecule Collision Theory*; Bernstein, R. B., Ed.; Plenum Press: New York, 1979.

(26) Desouter-Lecomte, M.; Remacle, F. *Chem. Phys.* **1992**, *164*, 11.

(27) Desouter-Lecomte, M.; Culot, F. *J. Chem. Phys.* **1993**, *98*, 7819.

(28) Remacle, F.; Desouter-Lecomte, M.; Lorquet, J. C. *Chem. Phys.* **1991**, *153*, 201.

(29) Desouter-Lecomte, M.; Jacques, V. *J. Phys. B: At. Mol. Opt. Phys.* **1995**, *28*, 3225.

(30) Desouter-Lecomte, M.; Lievin, J. *J. Chem. Phys.* **1997**, *107*, 1428.

(31) Someda, K.; Nakamura, H.; Mies, F. H. *Chem. Phys.* **1994**, *187*, 195.

(32) Someda, K.; Nakamura, H.; Mies, F. H. *Prog. Theor. Phys.* **1994**, *116*, 443.

(33) Rotter, I. *Rep. Prog. Phys.* **1991**, *54*, 635.

(34) Iskra, W.; Rotter, I.; Dittes, F. M. *Phys. Rev. C* **1993**, *47*, 1086.

(35) Rotter, I. *J. Chem. Phys.* **1997**, *106*, 4810.

(36) Peskin, U.; Reisler, H.; Miller, W. H. *J. Chem. Phys.* **1994**, *101*, 9672.

(37) Peskin, U.; Reisler, H.; Miller, W. H. *J. Chem. Phys.* **1997**, *106*, 4812.

(38) Lovejoy, E. R.; Kim, S. K.; Moore, C. B. *Science* **1992**, *256*, 1541.

(39) Moore, C. B.; Smith, I. W. M. *J. Phys. Chem.* **1996**, *100*, 12848.

(40) Barnes, R. J.; Dutton, G.; Sinha, A. *J. Phys. Chem.* **1997**, *101*, 8374.

(41) Wedlock, M. R.; Jost, R.; Rizzo, T. R. *J. Chem. Phys.* **1997**, *107*, 10344.

(42) Reid, S. A.; Reisler, H. *J. Phys. Chem.* **1996**, *100*, 474.

(43) Peskin, U.; Miller, W. H.; Reisler, H. *J. Chem. Phys.* **1995**, *102*, 8874.

(44) Fano, U. *Phys. Rev.* **1961**, *124*, 1866.